International Journal For Technological Research in Engineering
Volume 12 Issue 8 April-2025 ISSN (online) 2347-4718

DIRECT TORQUE CONTROL OF PERMANENT MAGNET SYNCHRONOUS MOTOR OPERATED ELECTRIC VEHICLE DRIVE BY USING FUZZY LOGIC BASED CONTROLLER

[1]Vikram Singh, [2]Dr. Anurag S.D. Rai
[1]Research Scholar, [2]Professor
Department of Electrical and Electronics Engineering
LNCT University, Bhopal, India

Abstract: ***The primary objective of this paper is to present an overview of DTC-SVPWM of PMSM driven electric vehicle (EV) drives. The DTC scheme is applied to PMSM driven EV units powered by three-phase supply. the Speed control of the PMSM driven EV is achieved through the Direct torque control technique and we are also improve our DTC control by using in conjunction with Fuzzy logic controller. DTC-FLC controller applying for tuning of PID controller. This study explores the fuzzy logic based controller is using with DTC-Space vector PWM. Additionally the research work includes the discussion on simulation-based results obtained after the simulation is done in MATLAB software.***

Index Terms: Fuzzy Logic Control (FLC), Direct Torque Control (DTC),Space Vector Pulse Width Modulation (SVPWM), Field Oriented control(FOC),Permanent Magnet Synchronous Motors (PMSM), MATLAB (2016)

I. INTRODUCTION

Permanent Magnet Synchronous Motors (PMSMs) are widely used in various applications due to their advantages over other types of industrial motors. These advantages include high power density, excellent speed control, and the ability to operate at higher speeds. As a result, PMSMs are commonly found in robotics and automation systems. Various torque control methods have been studied for PMSM drives, with two major control strategies being widely used: Field-Oriented Control (FOC) and Direct Torque Control (DTC).

Recently, the adoption of Direct Torque Control with Space Vector Pulse Width Modulation (DTC-SVPWM) in PMSM drives has increased, particularly for Electric Vehicles (EVs). This approach allows for rapid and efficient control of motor torque and stator flux with minimal implementation complexity. In DTC, stator voltage information is processed to select the appropriate voltage vector, while estimated torque is compared with stator voltage to minimize errors. While DTC-SVPWM offers fast dynamic response, its digital implementation is limited by issues such as high sampling requirements, variable switching frequency, and torque ripple. Furthermore, the limited application of voltage vectors can reduce torque control accuracy.

PMSMs are becoming more popular as energy-efficient alternatives to induction motors, especially for high-power applications like industrial robots and machine tools. Their compact design, high power density, and low maintenance requirements make them a preferred choice. The key benefits of PMSMs include high energy density, cost-effectiveness, good efficiency, favorable inertia ratio, and ease of maintenance, which contribute to their widespread use across different industries.

The widespread use of synchronous motors, especially PMSMs, is attributed to advances in vector control technologies. These technologies allow for independent torque and speed control, which minimizes torque ripple during phase transitions. However, operating at higher switching frequencies increases switching losses, reducing overall system efficiency. To address the nonlinear and coupled behavior of AC motors, specialized algorithms are needed to manage the variables. Field-Oriented Control (FOC) addresses these challenges by reducing torque variations and ensuring stable motor performance at a constant switching frequency. However, the performance of proportional-integral (PI) controllers used in FOC can be impacted by changes in parameters, load disturbances, and variations in speed.

In conclusion, PMSMs offer significant benefits, such as high efficiency and low maintenance, making them a popular choice for demanding industrial applications. However, the control methods used, particularly DTC-SVPWM, come with certain challenges, including torque ripple, variable switching frequency, and limitations in digital control implementation. Continued development of advanced control strategies is needed to overcome these limitations and enhance the performance of PMSMs in high-performance applications.

II. MATHEMATICAL MODELING OF PMSM

The PMSM has been represented through both the ABC and DQ models represent in fig. 1. These models make the assumption that the rotor flux remains constant and are concentrated along the d-axis. Additionally, it is considered that the stator winding has an equal number of turns per phase [8, 9].

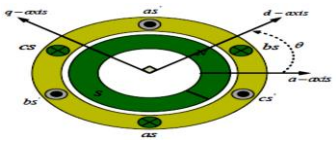

Figure 1.Surface Mounted PMSM

The rotational coordinate of the stator serves as the base for the x-y coordinate system, with the stator flux linkage oriented in the positive direction of the x-axis, as illustrated in Figure 2. Utilizing the stator flux (xy), rotor flux (dq), and stationary (DQ) frames allows for the representation of the rotor flux linkage (f) and stator flux linkage vector (s) of the PMSM.

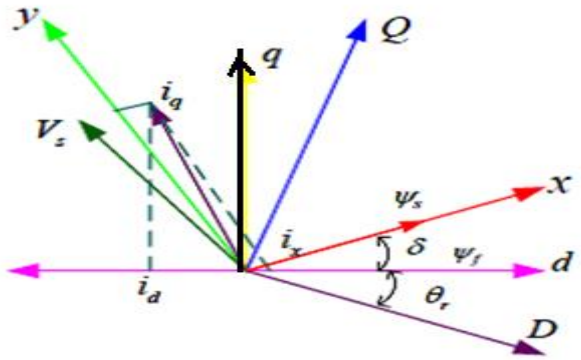

Figure 2.Flux linkage of stator and rotor

The symbol **δ** denotes the load angle between the stator and rotor flux linkages. Under stable conditions, **δ** remains constant. The stator motion reference frame and the stator flux linkage space vector Ψs are in phase along the x-axis [10, 11]. The Q-axis undergoes a counter clockwise rotation of 90 degrees from the D-axis, as depicted in Fig. 2. Let **θ**r represent the rotational electric angle of the rotor, and **θ**s be the rotational angle of the stator flux vector.

$$\omega_r = \frac{d\theta_r}{dt}$$

$$\theta_s = \theta_r + \delta$$

Stator flux linkage is given by

$$\Psi_s = L_s i_s + \Psi_{af} e^{j\theta r} \qquad (1)$$

Where L_s = Stator self-inductance

Ψ_{af} = Rotor permanent magnet flux linkage.

In rotor reference frame, the stator voltage equation (d-q reference frame) are given as [12, 13]

$$V_d = R_d i_d + \frac{d\Psi_d}{dt} - \omega_r \Psi_q \qquad (2)$$

$$V_q = R_q i_q + \frac{d\Psi_q}{dt} + \omega_r \Psi_d \qquad (3)$$

Where R is for resistance and subscript d & q for d-axis and q-axis.

$$R_d = R_q = R_s$$

A continuous Voltage source can be used to imitate the excitation of permanent magnets. The rotor current on the q-axis is zero. The flux linkage is then written.

$$\psi_q = L_q i_q \qquad (4)$$

$$\psi_d = L_d i_d + \psi_f \qquad (5)$$

ψ_f is the flux due to permanent magnet

$$\psi_f = L_m i_f \qquad (6)$$

L_m is mutual inductance between the rotor and stator windings.

The torque equation is obtained by the below Equation.

$$T_e = \frac{3}{2} P \left[\Psi_d i_q - \Psi_q i_d\right] \qquad (7)$$

III. DIRECT TORQUE CONTROL

The fundamental concept behind the DTC-SVPWM principle lies in the selection of appropriate voltage vectors based on the generated errors in torque and flux in fig. 3 [14, 15]. The difference between the actual flux and torque, as measured at the motor terminal and their respective set values is essentially termed as the flux and torque error. The torque expression is influenced by the interaction between the fluxes in the stator and rotor. To ascertain torque and flux ratings, we measure the stator voltage and current at the motor terminals, respectively.

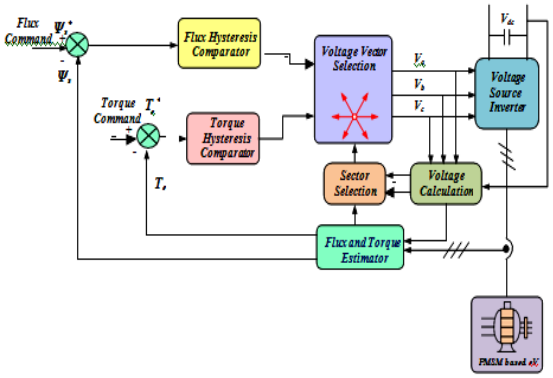

Figure 3.Speed Control of PMSM driven EV drive

Hysteresis comparators play a crucial role in governing the control of stator flux and torque. They give way an output that is subsequently utilized to select the optimal voltage vector for controlling the Voltage Source Inverter (VSI) from the set of six non-zero and two zero vectors. Each of the six switches is represented in binary form, with states 1 and 0 denoting their on and off positions, respectively. The combination of these binary states across the three branches results in a total of $2^{\wedge 3}$ = 8 switching states. With three switch configurations (S_1, S_2, S_3), one for each inverter leg as illustrated in Fig. 4, it becomes possible to realize every conceivable combination. In this example, the top switches of the voltage source inverter are denoted as S_1, S_2, and S_3. When the top switch is closed, it has a binary value of 1, while the bottom switch has a value of 0, and vice versa is representing in table 1. It is imperative that the

switch position on top is always opposite to the switch position on the bottom to prevent a short circuit in the power supply [16, 17].

The stator voltage space vector is given by :-

$$V_S=\frac{2}{3}*V_{dc}*(S_1+S_3^{ei2}\pi^{/3}+S_5^{ei4}\pi^{/3}) \quad (8)$$

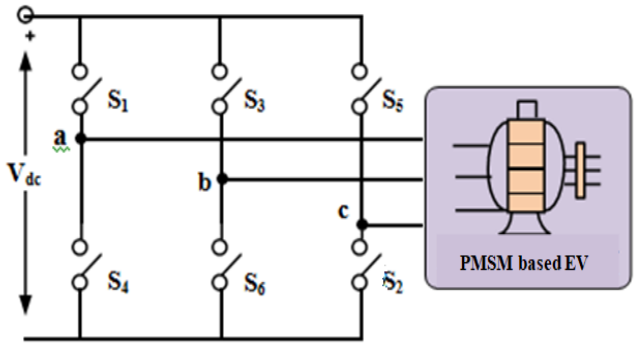

Figure 4.VSI Conned with PMSM Driven EVs Drive

Table 1: Switching Conditions & Space Vectors

Switching Condition	State	State SpaceVector
1,2,6On	1(100)	V_1
2,3,1On	2(110)	V_2
3,4,2On	3(010)	V_3
4,5,3On	4(011)	V_4
5,6,4On	5(001)	V_5
6,1,5On	6(101)	V_6
1,3,5On	7(111)	V_7
4,6,2On	8(000)	V_8

Our research work is going to be focused in three type of speed control approaches, when we are using DTC-SVPWM technique, Fuzzy logic controlled-DTC and PSO tuned DTC.

Case 1: DTC-SVPWM scheme of PMSM drove EVs Drive.

Case 2: Fuzzy Logic controlled DTC (FLC-DTC) scheme of PMSM Driven EVs Drive.

Case3: PSO Tuned DTC scheme of PMSM Driven EVs Drive

Case-1: In DTC-SVPWM (Direct Torque Control by using Space Vector Pulse Width Modulation) of PMSM driven Electric Vehicles (EVs) drive supplied by an SVPWM inverter ,when applying voltage in the vector's direction increases the magnitude of the stator current vector. When a voltage is applied on the stator side perpendicular to the flux vector, the flux vector inherently tends to rotate. However, the torque produced, whether it increases or decreases, depends on the direction of this rotation.

A space vector chosen from Table-1 represents the fundamental switching of all six switches in various configurations [18]. Figure-V visually depicts the concept of electromagnetic torque control for a three phase inverter. The entire vector space is segmented into six stator flux zones, each with a central point where all possible inverter voltage vectors can be positioned. The rotor flux vector is denoted by Ψr, and the stator flux vector is represented by Ψs. Fig. 5 also shows four voltage vectors labeled ΔΨs at the conclusion of the stator current vector. These six voltage vectors, namely V_1,V_2, V_3,V_4,V_5, and V_6 exert distinct effects on the stator current, illustrating how the current varies concerning the application of the voltage vector.

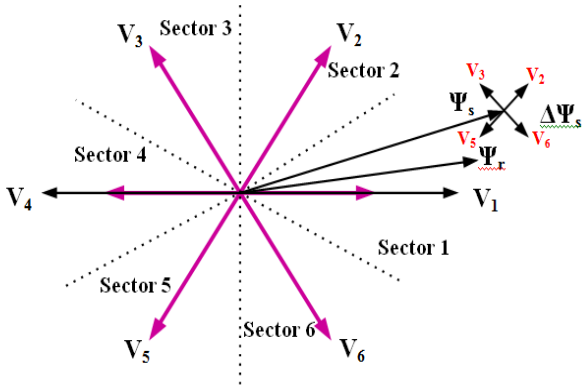

Figure 5.Torquecontrol for DTC-SVPWM inverter of PMSM Driven EVs Drive

Case 2: Fuzzy logic controlled DTC (FLC-DTC) of PMSM driven EV Drive

Fuzzy logic control are widely adopted in designing highly nonlinear controllers, is an analytical approach that attached human critical intellectual thought processes and information processing capabilities. When traditional control theory proves inadequate, the exploratory nature of fuzzy logic proves most effective [19]. Substituting a Fuzzy Logic Controller in DTC for a conventional controller can yield highly optimized outcomes across a broad spectrum of industrial applications, including the control of PMSM driven Electric Vehicles (EVs) drive. FLC exhibits near immunity to system disturbances and can handle extremely fuzzy input data without necessitating precise mathematical models. Furthermore, the existing system configuration typically requires minimal modification. Additionally, FLC-DTC contributes to cost-effective enhancements in the performance of current control mechanisms.

Fuzzy logic has been applied to the reference values of the speed control loop, and FLC-DTC has been integrated into the control scheme the dynamic performance of DTC-SVPWM control [20, 21]. The control rules follow a format such as "If (antecedent 1) and (antecedent 2) are true, then (consequent)," with a total of 49 rules developed in this structure. Tools like

Rules Viewer and Surface Viewer prove useful for visualizing the rules and regulations page. The determination of a can be accomplished through various estimation algorithms.

Conventional rules and concepts: -The essential components of control systems consist of implicit rules, conveyed through a series of linguistic statements within operational control systems. Conditional statements, like "if," are frequently employed to articulate specific knowledge assertions. Member functions are uniformly distributed across the entire system, and triangle functions are utilized to facilitate computations [22]. To enhance accuracy, the member functions are designed to be denser towards the initial part of each function, as illustrated in matlab-based figures shown in Fig. 6 (a, b, c).

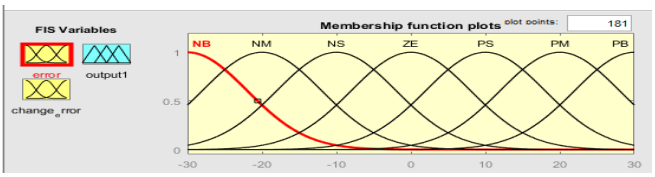

(a)

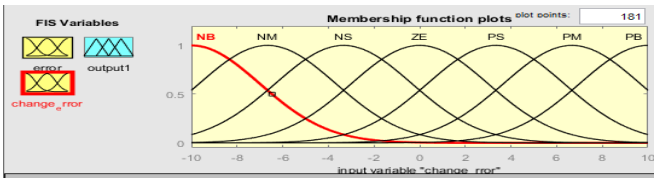

(b)

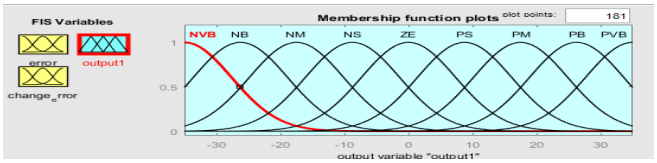

(c)

Figure 6.Wave form of membership function for (a) Error (b) Change in error (c) Output

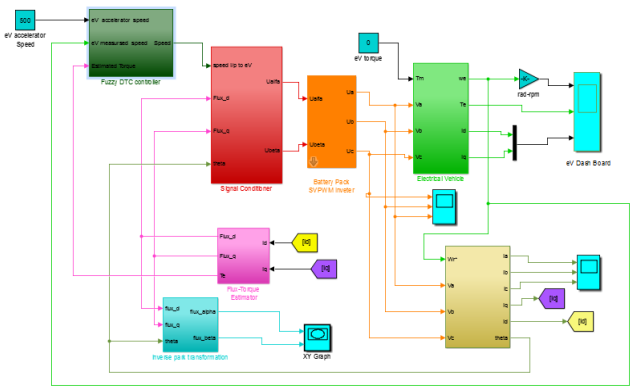

Figure 7.MATLABmodel of PMSM Driven EVs by using FLC-DTC

Fig. 7 shows that the DTC scheme of PMSM driven EV unit by employing a Fuzzy Logic Controller. This control scheme integrates closed-loop speed and torque control. The current feedback loop obtains measured three-phase voltages (V_a, V_b, and V_c) from the rotor circuit [23, 24] And subsequently, these Voltages are transformed into DC components (U_d and U_q) through separate Park's transformations. The FLC, working in tandem with the current directions of the d, q, and i_e axes, fine-tunes the difference between the reference velocity and the actual velocity.

For each DC component, i_{dref} and i_{qref}, a dedicated FLC controller is employed to control both i_d and i_q. Within the FLC, the speed error (ω_e) and the speed shift error (dw_e/dt) function as two fuzzy input variables represent in fig. 8. The regulated DC current generates three-phase stator currents, and these voltages are then fed into the voltage source inverter to generate the necessary torque and speed. ΔI_w represents the FLC output, constituting a part of the overall product. Two information factors are addressed by seven membership functions, encompassing zero (ZE), Positive very big(PVB),small positive (PS), medium positive (PM), negative small (NS), negative large (NB), negative medium (NM),negative very big (NVB) and large positive (PB).

$$W_e(y) = w_{reff}(y) - w(y)$$

$$c_{we} = w_e(y) - w_e(y\text{-}1)$$

These w_e and c_{we} are partitioned by scaling factor SF and SQ separately to change over the sign in per unit esteems the adequacy of result of FLC is given as:

$$I_w(y) = I_w(y\text{-}1) + \Delta I_w$$

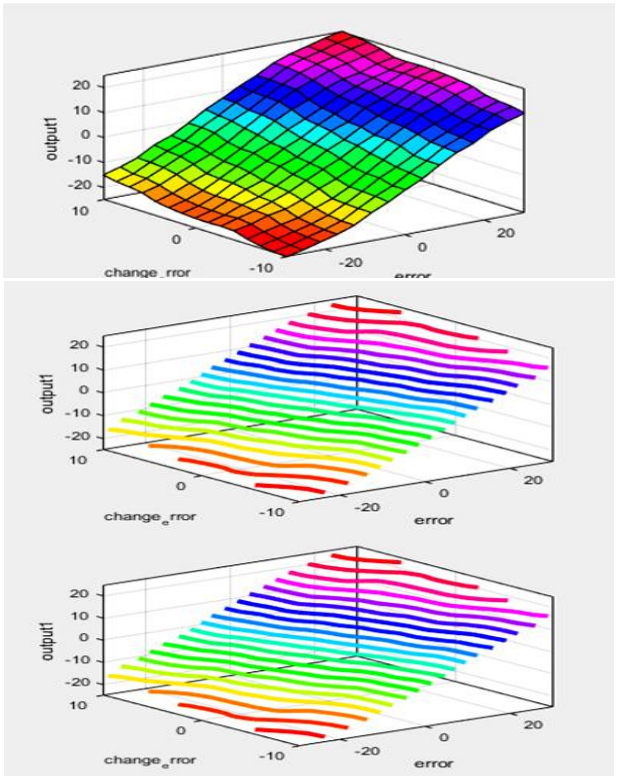

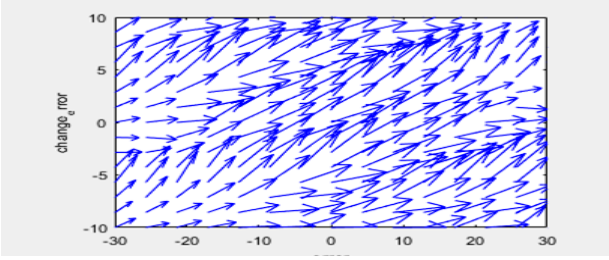

Figure 8.Generated Surface Viewer using FLC-DTC

Case3: **PSO tuned DTC of PMSM driven EVs**

In process industries, nonlinear processes are commonplace, and stabilizer designs are often employed to enhance production rates. This research work utilizes the PSO algorithm for fine-tune the Proportional-Integral-Derivative (PID) controller for stable and time-delayed unstable process models. The inertial parameters are assigned fixed weights in the search space with dimensions (c, R_1, and R_2). A comparison is made between various inertial weights, including 0.5, 0.75, and 1. The results indicate that the proposed PSO tuned DTC approach facilitates the achievement of improved controller settings with minimal iterations.

The suggested method is implemented in real-time within the PSO tuned DTC of speed control system, utilizing both simulation and real-time data. The study reveals that the PSO algorithm operates effectively, as demonstrated by the examination of static and non-stationary process models. Additionally, motor motion detection challenges are addressed in this work through the use of the Bird swarm optimization algorithms. The PSO algorithm, proposed by Kennedy and Eberhardt in 1995, continues to prove its efficacy in optimizing controller parameters for complex and dynamic processes.

$$F = Mp + IAE$$

Objective function is used to minimize F, Where Mp = Maximum Over shoot and IAE is lowest modified integral time of absolute error

$$IAE = \int_0^t e(T)\, dt$$

PID Controller tuning by using PSO: The objective of the controller design process is to minimize the considered objective function by identifying the optimal values for the parameters of the controller within the defined search space.

PSO Flow Chart: The following flow chart of PSO tuned DTC is representing in fig. 9**.**

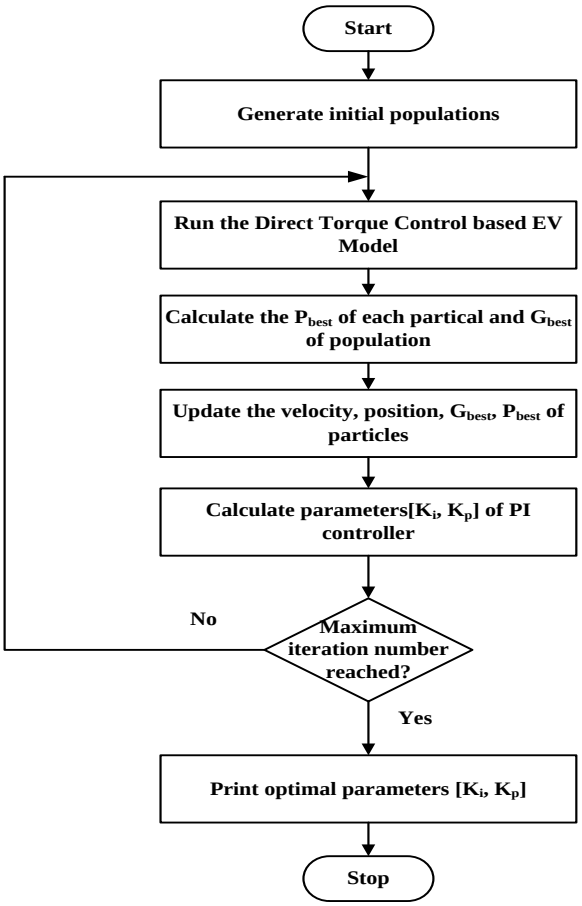

Figure 9.Flow Chart of PSO Tuned DTC

IV. SIMULATION RESULTS

The result analysis involves that comparing of the characteristics of PMSM driven Electric Vehicles fewer than three different controllers: DTC-SVPWM controller, FLC-DTC controller, and PSO tuned DTC controller. The comparison is conducted with fixed speed reference at 500 rpm and different load conditions, specifically 0 Nm, 5 Nm, 10 Nm, and 15 Nm. The analysis considers different simulation times until the actual speed reaches the reference speed. This comparison aims to evaluate and understand the performance of particular controller under varying load conditions .This analysis seeks to understand how the DTC performs under different load conditions within the specified speed range of 500 rpm. The investigation may include examining variables such as torque response, speed accuracy, and overall system stability to gain insights into the controller's effectiveness in managing varying loads at the specified speed range.

Case-I Analyzing the DTC-Space Vector Pulse Width Modulation (DTC-SVPWM) controller involves assessing its performance at a reference speed of 500 rpm under different loading conditions. The analysis includes studying the

system's response to changes in applied load, specifically when the load is varied from 0 Nm, 5 Nm, 10 Nm, to 15 Nm.

S.No	Reference speed (rpm)	Actual speed (rpm)	Load torque (Nm)	Ripple (%)	Settling time (ms)	Rise time (ms)	Overshoot %	Undershoot %
1	500	500	0	0	576	1.854	13.068	3.202
2	500	498	50	0.4	949	2.060	3.64	11.123
3	500	494.1	10	1.2	1457	1.548	4.177	2.592
4	500	495.7	15	0.86	2129	3.6	-1.3	2

Case-II: Analyzing the Fuzzy logic controlled DTC controller involves assessing its performance at a reference speed of 500 rpm under different loading conditions. The analysis includes studying the system's response to changes in applied load, specifically when the load is varied from 0 Nm, 5 Nm, 10 Nm, to 15 Nm.

S.No	Reference speed (rpm)	Actual speed (rpm)	Load torque (Nm)	Ripple (%)	Settling time(ms)	Rise time(ms)	Overshoot %	Undershoot %
1	500	500	0	0	122	0.512	1.851	11.29
2	500	497	5	0.6	945	1.835	40.14	28.89
3	500	494.1	10	1.2	534	1.756	36.56	30.95
4	500	490.7	15	2	2.398	2.398	23.144	28.144

Case-III: Analyzing the PSO tuned DTC controller involves assessing its performance at a reference speed of 500 rpm under different loading conditions. The analysis includes studying the system's response to changes in applied load, specifically when the load is varied from 0 Nm, 5 Nm, 10 Nm, to 15 Nm.

S.No	Reference speed (rpm)	Actual speed (rpm)	Load torque (Nm)	Ripple (%)	Settling time(ms)	Rise time(ms)	Overshoot %	Undershoot %
1	500	500	0	0	747	544	1.96	2.151
2	500	500	5	0	1049	1700	21.34	35.32
3	500	498	10	0.4	1100	2341	4.737	31.24
4	500	497	15	0.6	1128	3313	8.152	12.138

Case 1:-Results of DTC-SVPWM Controller: -It appears that the machine achieves the reference speed of 500 rpm in 0.747 seconds at no load condition. The reference speed is set at 500 rpm and the estimated simulation time for the machine is 0.6 seconds. This information suggests that the machine efficiently reaches the specified speed within a relatively short duration, showcasing its performance under the given condition shown in fig. 10.

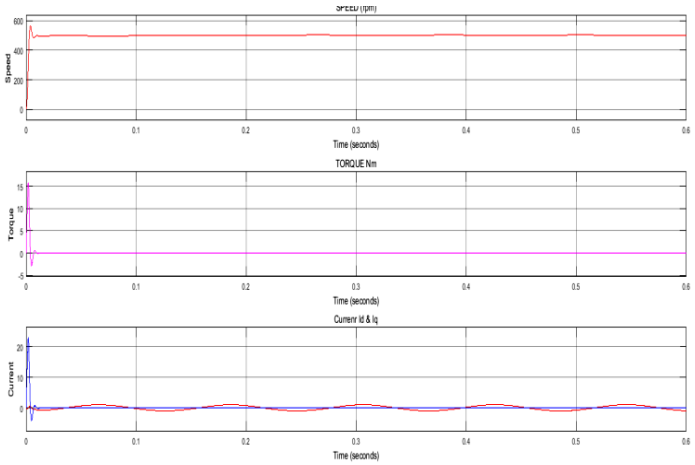

Figure 10: Results of DTC-SVPWM Controller, Speed 500 rpm, at no load condition &simulation time is 0.56ms

Case 2: Results of Fuzzy Logic controlled DTC controller: In the scenario where the reference speed is set at 500 rpm with No Load condition, the machine records the actual speed. The simulation time is 2.5 seconds, and the system achieves stability with an estimated settling time of 0.12seconds. This information provides insights into how the machine responds and stabilizes when aiming to reach and maintain a speed of 500 rpm under the specified conditions shows in fig. 11.

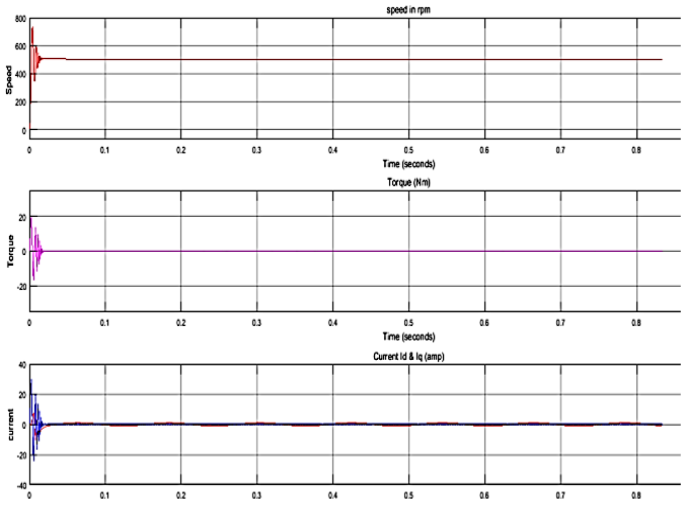

Figure 11. Result of Fuzzy DTC controller Speed 500 rpm, Torque is 0 nm, running time is 0.56ms

Case3: Results of PSO Tuned DTC Controller: -It seems that the machine successfully attains the actual speed when the reference speed is set at 500 rpm with no load torque. The simulation time is set to 2 seconds, and the estimated settling time is recorded as 0.16 milliseconds. This data provides valuable insights into the machine's performance, demonstrating its ability to reach and stabilize at the desired speed within the specified conditions shows in fig. 12.

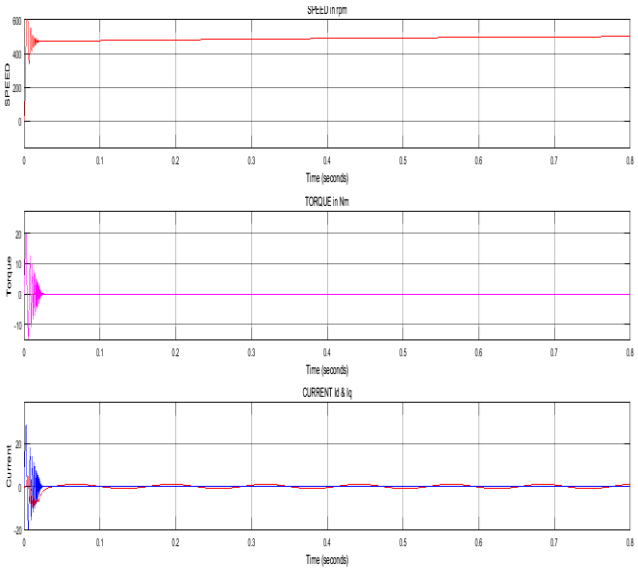

Figure 12. Results of PSO Tuned DTC Controller at reference Speed of 500 rpm, at no load condition &running time is 0.8ms

V. CONCLUSION

The provided results indicate that the system is stable, and the machine successfully achieves the reference speed when employing a DTC-SVPWM controller within an appropriate settling time. Although the machine attains the desired speed and experiences reduced speed ripple, some initial disturbances are observed during the starting phase of operation. Moreover, it is noted that the DTC-SVPWM controller exhibits a slower speed control response when compared to both the fuzzy Logic Controlled DTC controller and the PSO Tuned DTC controllers. The utilization of the Particle Swarm Optimization (PSO) algorithm, with various inertia weights, proves effective in achieving the research objective of optimizing controller parameters. The reference speed is increased, and the constant inertial mass method ensures good parameter accuracy.

In summary, the study suggests that the fuzzy Logic Controlled DTC controller and PSO Tuned DTC controllers outperform the DTC-SVPWM controller in terms of speed control response. This highlight the advantages of optimization techniques such as the PSO algorithm in enhancing the performance of motor speed control systems, ultimately leading to improved speed control and reduced disturbances during operation.to the provided results, the system is stable and the machine achieves reference speed when using a DTC-SVPWM controller at the appropriate setting time. While the machine has reached its proper speed and the speed ripple has decreased, there are still some initial disturbances are observed during the starting phase of operation. Additionally, it is discovered that the

REFERENCES

[1] NiuB. Wang, Babel A. S., Li K. and StrangasE. G., "Comparative Evaluation of DTCStrategies for Permanent Magnet Synchronous Machines" in *IEEE Trans. Power Electron*, vol. 31, no. 2, pp. 1408–1424, 2016

[2] Li, J., Yu, J.J., Chen, Z., 2013. A Review of Control Strategies for Permanent Magnet Synchronous Motor Used in Electric Vehicles. AMM 321–324, 1679–1685.

[3] MerzougM. S., and Naceri F., "Comparison of field-oriented control and DTCfor permanent magnet synchronous motor (PMSM)" *World Academy of Science, Engineering and Technology*, vol. 45, pp. 299–304, 2008

[4] Ahmed Abdelsalam, Quntao An, and Li Sun., "DSP-Based implementation of permanent magnet synchronous motor drives for EV/HEV applications." *proc. 16th International Middle East Power Systems Conference (MEPECON'14)*, pp. 23–25, 2014.

[5] Imura A., Takahashi T., Fujitsuna M., Zanma T., and Ishida M.. "Instantaneous-current control of PMSM using MPC: Frequency analysis based on sinusoidal correlation." In *IECON 2011 — 37th Annual Conference of the IEEE Industrial Electronics Society*, pp. 3551–3556, Nov 2011.

[6] Zhang X., Zhang L., and Zhang Y., "Model predictive current control for PMSM drives with parameter robustness improvement," *IEEE Trans. Power Electron*, vol. 34, no. 2, pp. 1645–1657, Feb. 2019.

[7] ShimaokaMasahiro; DokiShinji. "Design of search space for improving the steady current control performance of PMSM current control system based on model predictive control." *Electrical Engineering in Japan*, vol. 214, no. 2, p. e23303, 2021.

[8] PreindlM. andBolognaniS.. "Model predictive DTCwith finite control set for PMSM drive systems, part 1: Maximum torque per ampere operation." *IEEE Transactions on Industrial Informatics*, vol. 9, no. 4, pp. 1912–1921, Nov 2013.

[9] Ahmed Abdelsalam A., Kim Jung-Su, and Lee Young Il. "Model predictive torque control of PMSM for EV drives: A comparative study of finite control set and predictive dead-beat control schemes." *Eighteenth International Middle East Power Systems Conference (MEPCON)*, IEEE, pp. 156–163, 2016.

[10] Abu-Rub H., Malinowski M., and Al-Haddad K., "*Power Electronics for Renewable Energy Systems, Transportation and Industrial Applications*." Hoboken, NJ, USA: Wiley, 2014.

[11] I. Takahashi and T. Nogushi, "A New Quick-Response and High-Efficiency Control Strategy of Induction Motor," IEEE Transactions on Industry Applications, Vol. 22, No. 5, 1986, pp. 820-827.

[12] M. Depenbrock, "Direct self-control (DSC) of inverter fed induction machine," 1987 IEEE Power Electronics Specialists Conference, 1987, pp. 632-641.

[13] Rong-Maw Jan, Chung-Shi Tseng, Ren-Jun Liu, Robust PID control design for permanent magnet synchronous motor: A genetic approach, Electric Power Systems Research,Volume 78, Issue 7, 2008, Pp. 1161-1168.

[14] K. Suman and A. T. Mathew, "Speed Control of Permanent Magnet Synchronous Motor Drive System Using PI, PID, SMC and SMC plus PID Controller," 2018 International Conference on Advances in Computing, Communications and Informatics (ICACCI), 2018, pp. 543-549, doi: 10.1109/ICACCI.2018.8554788.

[15] SweetyKumari, Sonali Raj, Ramesh Kumar. (2020) Performance Review of Fractional Order PID (FOPID) Based Controllers Employed in Brushless DC Motor. *2020 International Conference on Power Electronics &IoT Applications in Renewable Energy and its Control (PARC)*, 192-197.

[16] RabieiAliet al., "Improved maximum-torque-per-ampere algorithm accounting for core saturation, cross-coupling effect, and temperature for a PMSM intended for vehicular applications." *IEEE Transactions on Transportation Electrification*, vol. 2, no. 2, pp. 150–159, 2016.

[17] Choi, Han Ho, Hong Min Yun, and Yong Kim. "Implementation of evolutionary fuzzy PID speed controller for PM synchronous motor." IEEE Transactions on Industrial Informatics 11.2 (2015): 540-547.

[18] Jung, Jin-Woo, et al. "Adaptive PID speed control design for permanent magnet synchronous motor drives." IEEE Transactions on Power Electronics 30.2 (2015): 900-908.

[19] S. K. Suman, M. K. Gautam, R. Srivastava and V. K. Giri, "Novel approach of speed control of PMSM drive using neural network controller," 2016 International Conference on Electrical, Electronics, and Optimization Techniques (ICEEOT), 2016, pp. 2780-2783, doi: 10.1109/ICEEOT.2016.7755202.

[20] L. YujieandC. Shaozhong, "Model reference adaptive control system simulation of permanent magnet synchronous motor,"

2015 IEEE Advanced Information Technology, Electronic and Automation Control Conference (IAEAC), 2015, pp. 498-502, doi: 10.1109/IAEAC.2015.7428603.

[21] R. K. Mahto and A. Mishra, "Self-Tuning Vector Controlled PMSM Drive Using Particle Swarm Optimization," 2020 IEEE First International Conference on Smart Technologies for Power, Energy and Control (STPEC), 2020, pp. 1-5, doi: 10.1109/STPEC49749.2020.9297764.

[22] N. R. Abjadi, J. Soltani, M. Pahlavaninizhad and J. Askari, "A nonlinear adaptive controller for speed sensorless PMSM taking the iron loss resistance into account," 2005 International Conference on Electrical Machines and Systems, 2005, pp. 188-193 Vol. 1, doi: 10.1109/ICEMS.2005.202510.

[23] Q. Zhu and P. Zhang, "A novel reaching law based on integral sliding mode control of permanent magnet synchronous motors," 2013 25th Chinese Control and Decision Conference (CCDC), 2013, pp. 4646-4651, doi: 10.1109/CCDC.2013.6561774.

[24] L. Pohl and L. Buchta, "$\mathscr{H}\infty$ tuning technique for PMSM cascade PI control structure," 2016 6th IEEE International Conference on Control System, Computing and Engineering (ICCSCE), 2016, pp. 119-124, doi: 10.1109/ICCSCE.2016.7893556.

[25] S. Hassaine, S. Moreau, S. Gherbi, M. Sedraoui and B. Mazari, "Real time implementation of a robust controller for PMSM drive system using H∞ norm," IECON 2012 - 38th Annual Conference on IEEE Industrial Electronics Society, 2012, pp. 1976-1981, doi: 10.1109/IECON.2012.6388899.